Molecular Crystals and Liquid Crystals
Publication details, including instructions for authors and subscription information:
http://www.tandfonline.com/loi/gmcl16

Photoconduction in Phenazine Single Crystals in the Regions of Singlet and Triplet Absorption

M. Samoc [a] [b], J. B. Webb [a] & D. F. Williams [a]

[a] National Research Council of Canada, Ottawa, Ontario, Canada, K1A OR6

[b] 1979-80. NRCC Research Associate, Institute of Organic and Physical Chemistry, Wroclaw Technical University, Wroclaw, Poland

Version of record first published: 21 Mar 2007.

To cite this article: M. Samoc , J. B. Webb & D. F. Williams (1980): Photoconduction in Phenazine Single Crystals in the Regions of Singlet and Triplet Absorption, Molecular Crystals and Liquid Crystals, 62:3-4, 201-212

To link to this article: http://dx.doi.org/10.1080/00268948008084022

Mol. Cryst. Liq. Cryst., 1980, Vol. 62, pp. 201-212
0026-8941/80/6204-0201$06.50/0

Printed in the U.S.A.

Photoconduction in Phenazine Single Crystals in the Regions of Singlet and Triplet Absorption

M. SAMOC,† J. B. WEBB, and D. F. WILLIAMS
National Research Council of Canada, Ottawa, Ontario, Canada K1A OR6.

(*Received April 14, 1980*)

The photoconductivity of phenazine crystals has been measured as a function of temperature and wavelength of excitation. In the singlet absorption region it appears that only free electrons are generated, and the overall generation process has an activation energy which is independent of the singlet absorption process. Photoconduction in the triplet absorption region is primarily due to hole detrapping; the photoconduction spectra show the structure of singlet-triplet absorption.

1 INTRODUCTION

A considerable effort has recently been made to elucidate the various mechanisms of carrier photogeneration and transport in molecular solids. The results of these studies could be of great importance because of the possible practical use of the materials in question.

It is now generally agreed that the photogeneration of carriers in molecular crystals (e.g. anthracene) may be described by a model similar to that proposed by Onsager.[1] This model, which has been found to be appropriate for description of photogeneration in inorganic solids, like, e.g., amorphous selenium, has to be generalized to account for the possibility of rapid dissipation of excess energy of the excited state, being the precursor of the pair of generated charges, via internal conversion, as pointed out by Hong and Noolandi.[2] This process, facilitated by the presence of various vibrational levels, occurs within the time periods of the order of 10^{-12} s and may lead

---

† 1979–80. NRCC Research Associate, permanent address: Institute of Organic and Physical Chemistry, Wroclaw Technical University, Wroclaw, Poland.

both to a substantial decrease of the overall efficiency of the photogeneration process, and, unlike in, e.g., amorphous selenium,[3] to the apparent independence of the thermalization length on the wavelength of the exciting light.

The experimental confirmation of the Onsager model, or indeed any of the other suggested theoretical models is difficult; it is hampered by the well-known factors influencing the wavelength, electric field and temperature dependences of the photocurrent, i.e. surface generation, recombination and trapping of charges, the latter being among the most important factors and certainly of great importance in organic materials.

The present paper is concerned with the mechanisms of photogeneration of charges in single crystals of α-phenazine. We have studied the steady-state photoconductivity in the regions of singlet and triplet absorption. The results are complementary to a separate study[4] in which pulsed photoconductivity in phenazine via one photon and two-photon absorption was investigated. Phenazine, the 9–10 diaza-anthracene was chosen for these studies for many reasons. The material itself is easily purified by zone refining, and its crystal structure is similar to that of anthracene. Also because the electronic levels of the phenazine molecule include, besides a $\pi\pi^*$ level, similar to that of anthracene, a lower-lying $n\pi^*$ state, characterized by a much lower absorption coefficient than that of the $\pi\pi^*$ state.[5,6]

Photoconductivity of phenazine was first investigated by Kleinerman *et al.*,[7] and then Itoh[8,9] who studied the photoconductivity spectra and temperature dependences of the photocurrent. The results of Itoh are in apparent disagreement with the generalized Onsager model since this author found a remarkable dependence of the photoconductivity activation energy on the wavelength of the exciting light.

2 EXPERIMENTAL

Single crystals of phenazine were grown by the Bridgman method from sublimed and zone refined materials. Single crystal platelets of various thicknesses were cut from the boules, parallel to the bc cleavage plane. These crystals were then mounted in a nitrogen flow dewar, with electrical contacts provided by the press-fit of conducting quartz [indium tin oxide covered, 20 Ω/□] and either brass or silver paste. The photoconductivity excitation was provided by a 2.5 kW xenon arc passed through a Chromatex grating monochromator [0.75 m, dispersion ~10 Å/mm]. The monochromatic output intensity was calibrated against a Hewlett Packard 8330 A flux meter. High-intensity light from a Spectra Physics argon laser [10 watts cw] was also occasionally used for excitation.

The measurements of the photocurrents were made with the crystals either in nitrogen or vacuum, the crystal temperatures being measured by a simple thermocouple.

3. EXPERIMENTAL RESULTS

A) Photocurrents in the region of singlet absorption

The spectral dependence of photocurrents was found to be similar to that given by Itoh.[8,9] Figure 1 shows typical photoconductivity action spectra of phenazine corrected for the variations of the intensity of the monochromatized light. The corrections have been made assuming a linear dependence of the photocurrent on the light intensity, because, such dependences were observed (see Figure 2) for the whole spectral range investigated. Only at very high light intensities did substantial deviations from the linear dependences occur. A striking feature of the spectra given in Figure 1 is the

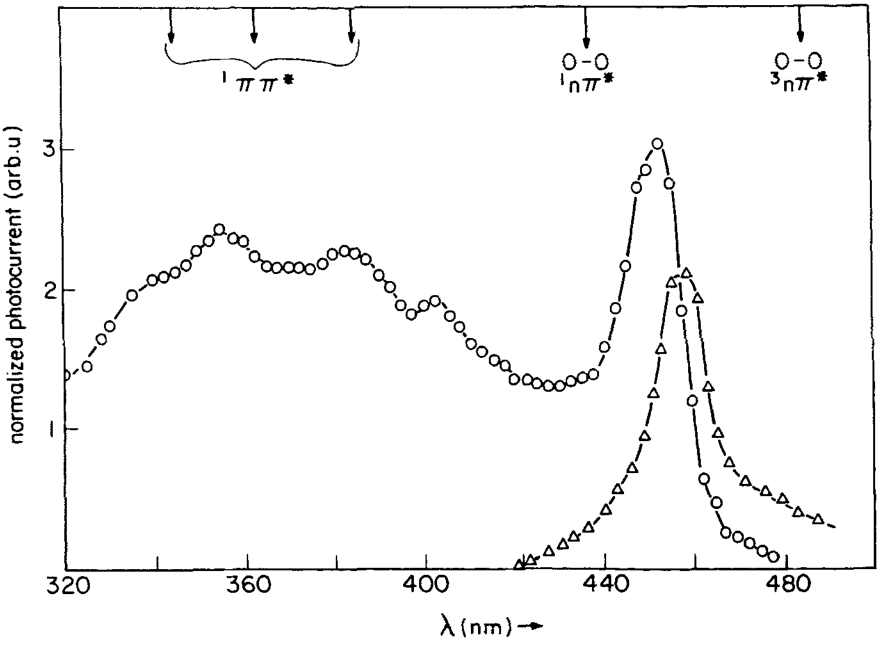

FIGURE 1 Normalized photocurrent spectra for a phenazine crystal (thickness $L = 0.7$ mm, voltage = 300 V). Circles denote negative photocurrent and triangles positive photocurrent. Arrows indicate positions of absorption maxima. $\pi\pi^*$ absorption—solution spectra after Ref. 5. $^1n\pi^*$ absorption—cryst. spectra after Ref. 12. $^3n\pi^*$ absorption—cryst. spectra after Clarke and Hochstrasser.[10]

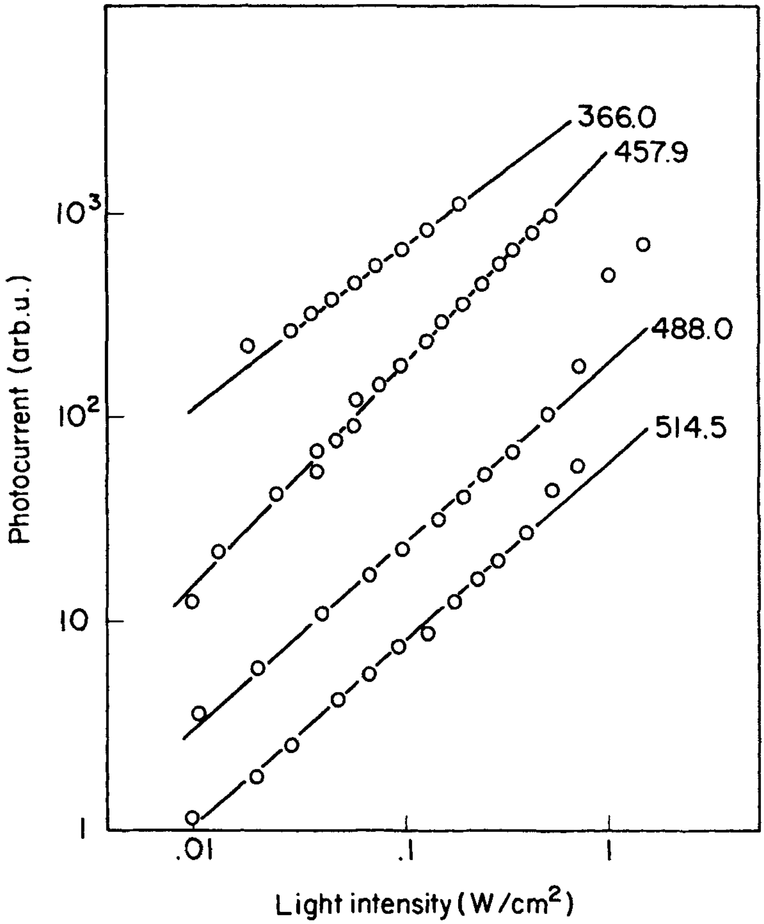

FIGURE 2 Intensity dependences of the photocurrent at wavelengths marked in the figure. Slopes of the straight lines are 0.77, 1.04, 0.88 and 0.87 for the wavelengths 366.0, 457.9, 488.0 *anf 514.5 nm, respectively.*

difference between photocurrents observed with positive and negative polarities of the irradiated surface. In the range of strong $\pi\pi^*$ absorption, virtually no positive photocurrent could be observed, whereas in the range of $n\pi^*$ absorption, positive and negative photocurrent spectra match each other more or less having a peak near 450–460 nm. This peak, however does not correspond exactly to the position of the $n\pi^*$ absorption maximum. The intensities of peaks in the spectra, as well as their positions, were found to vary slightly depending on sample history, i.e. on previous irradiation of the sample with a particular wavelength. This phenomenon will be discussed later. More

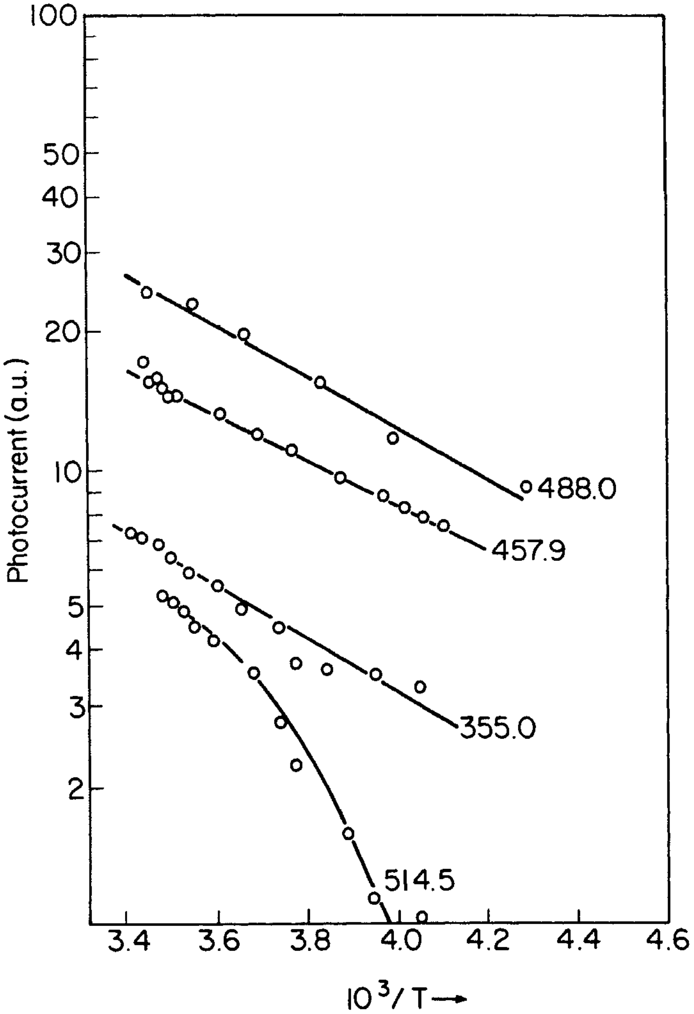

FIGURE 3 Temperature dependences of the photocurrent at wavelengths marked in the figure.

importantly, the position of this main peak (i.e. 450 nm) was found to shift to longer wavelengths for thicker samples, the shift being as large as 10 nm for an increase in thickness by the factor of four.

Typical temperature dependences of photocurrents are given in Figure 3. It can be seen that the activation energies of photocurrents are *ca* 0.12 eV, however, at longer wavelengths the dependences can no longer be considered exponential, and, apparently, attempts to interpret them as thermally activated would yield much higher activation energies, as it has been reported by Itoh.

B. Photocurrents in the region of triplet absorption

Studies of the long wavelength tail of the photocurrent spectra revealed some structure which can be attributed to the spin forbidden $S_0 \rightarrow T$ transition. Figure 4 shows examples of spectra in which a vibrational structure of the singlet-triplet absorption can be roughly seen. The intensities of maxima increase markedly when the sample is irradiated with the light in the range of strong absorption prior to recording a spectrum. Positions of the maxima coincide very well with the positions of absorption lines of singlet-$\pi\pi^*$ triplet transition given by Clarke and Hochstrasser.[10] It should be emphasized here that photocurrent spectroscopy seems to be a very sensitive tool

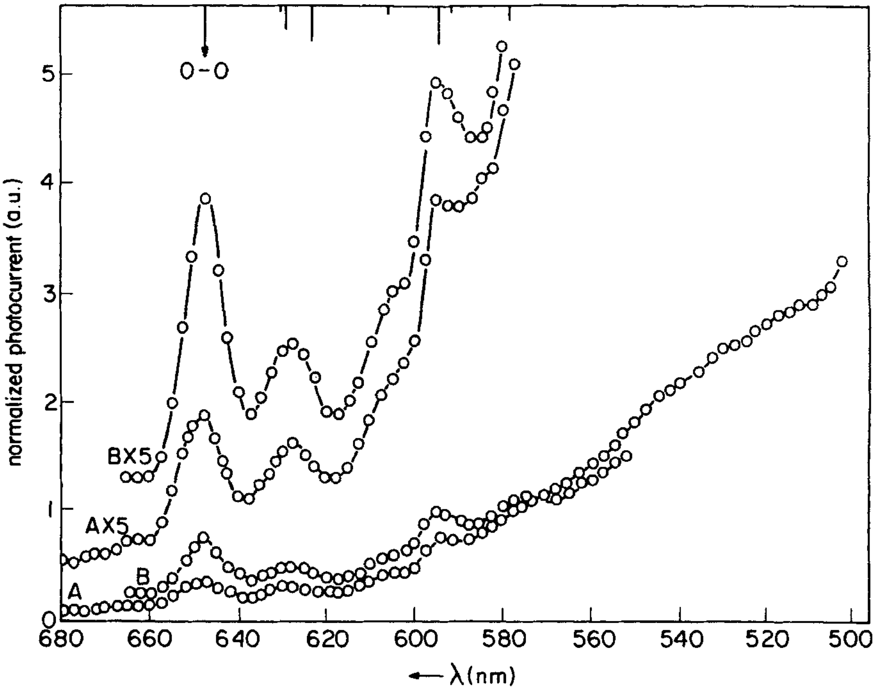

FIGURE 4 Normalized photocurrent spectra in the region of triplet absorption. The photocurrent scale is *ca* 10^2 times enlarged as compared to that of Figure 1. Spectrum A was obtained for a virgin sample, and spectrum B after several minutes of irradiating the sample within the region of singlet absorption. The arrow denotes the O–O $^3\pi\pi^*$ absorption and the vertical sections denote the positions of vibrational maxima in the triplet absorption spectrum (the height of these describes qualitatively the strength of a transition). Data are taken from Ref. 10.

in detection of a weak triplet absorption. One of the advantages of this form of spectroscopy[11] is that although similar absorption intensities may be readily due to impurities in a crystal, large lifetimes of triplet excitons make them efficient species for detrapping of carriers if a sample is previously excited to produce a large number of trapped charges. Impurity absorption does not seem to be efficient in detrapping of charges.

No structure due to the absorption by the $n\pi^*$ triplet could be observed —according to Hochstrasser and Marzzacco[12] the $^3n\pi^*$ absorption occurs close to the $^1n\pi^*$ absorption so that absorption peaks are seen as broad humps on the singlet absorption tail only.

4 DISCUSSION

Many different photogeneration paths may take place in molecular solids. One can distinguish between intrinsic and extrinsic processes, bulk and surface generation, one or two photon (exciton) processes, etc., by a close examination of the absorption coefficient and light intensity dependences of photocurrent. The results presented in Section 3 clearly indicate that generation of charges in phenazine involves a single photon or exciton. Since the energy of a singlet $\pi\pi^*$ exciton (*ca* 3.2 eV) and, of an $n\pi^*$ singlet exciton (*ca* 2.7 eV) are both much lower than the energy gap between conduction and valence bands (which can be estimated as *ca* 4.1 eV, taking data from compilation by Karl and Probst[13] one cannot expect an exciton to dissociate giving a pair of free charges. Such a process would demand a large amount of thermal energy to be transferred to an exciton, thus making it completely improbable taking into account relatively short lifetimes of singlet excitons. An energy balance can be established without invoking the help of lattice vibrational energy if an exciton dissociates close to a centre which itself acts as a deep electron or hole trap.

Examination of curves in Figure 1 gives immediately the suggestion that hole trapping is involved in photogeneration in phenazine. In the region of strong absorption no positive photocurrent is detected, because of a very short mean-free path of free electrons generated close to the surface. A symbatic behaviour of the negative photocurrent action spectrum in the region of $\pi\pi^*$ absorption maxima indicates that surface hole traps may play an important role in generation of carriers. However, a bulk process has to be considered to explain an appearance of a peak at *ca* 450 nm. To discuss the origin of this maximum which is not necessarily related to the absorption maximum of the $^1n\pi^*$ $S_2 \rightarrow S_0$ transition, it should be noted that the photogeneration process involving production of trapped holes and free electrons should give rise to the gradual increase in concentration of recombination centres (trapped holes) for electrons in the sample. If one takes into account that holes are thermally detrapped rather inefficiently (at room temperature the residence time of a hole in a 1 eV deep trap may be of the order of hours) then some equilibrium may be considered to exist between the rates of generation of both charges, recombination of electrons with trapped holes and detrapping of holes by photons and excitons. The steady-state concentration of trapped holes may be so large that besides the primary recombination (i.e. the recombination of an electron with its countercharge created in the exciton dissociation process—this recombination rate is discussed in the Onsager model), the secondary recombination may substantially reduce the overall efficiency of photogeneration.

A simple model taking into account the secondary recombination (see Appendix) predicts that for moderate recombination rates the photocurrent vs. absorption coefficient curve should exhibit a maximum at a point where the product $\varepsilon \cdot L$ (ε being the absorption coefficient and L the sample thickness) is of the order of unity (see Figure 5). Although the curves in Figure 5 can only be considered as a qualitative illustration of the concept, the general conclusions which can be drawn from the analysis of the numerical results

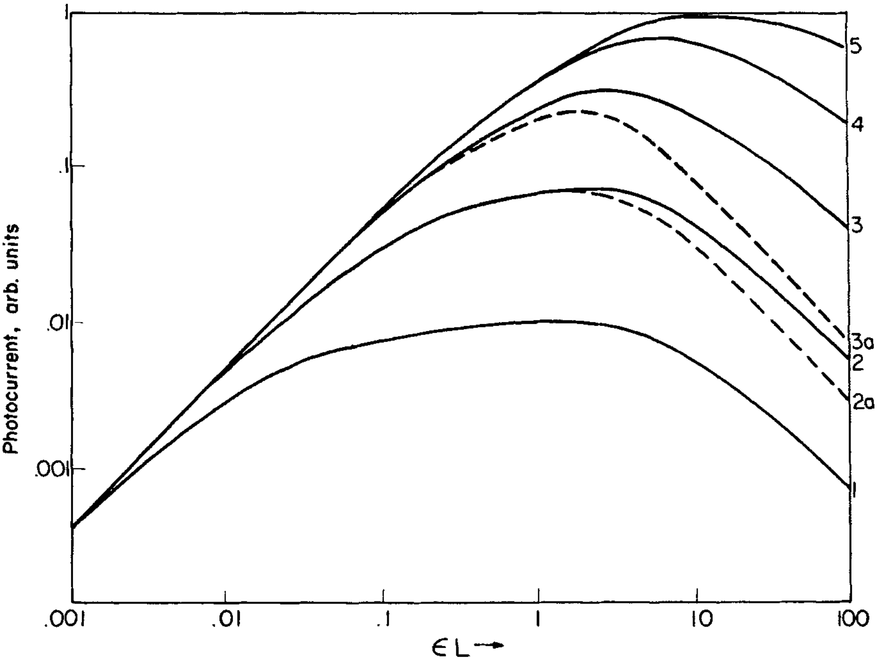

FIGURE 5 Photocurrent dependence on the absorption coefficient calculated from Eq. (5). The parameter A (Eq. 8, Appendix) was taken 0.01, 0.1, 1, 10 and 10^3 for curves 1–5, respectively. Dashed lines (2a and 3a) denote the photocurrent for positive polarity.

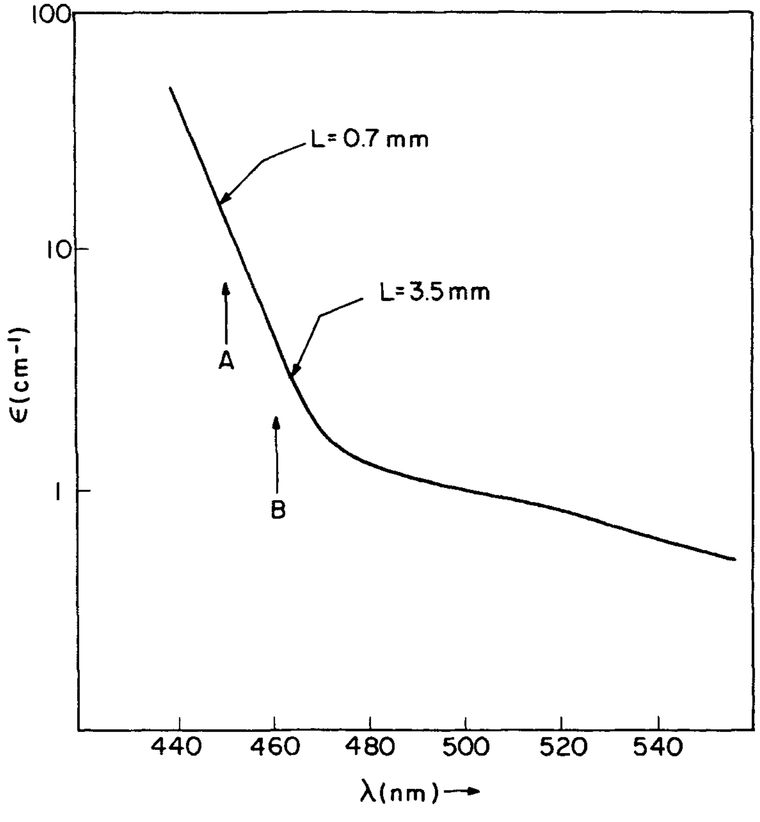

FIGURE 6 The absorption edge of phenazine (from room temperature absorption spectra of evaporated film). Arrows A and B denote positions of photocurrent maxima found for samples 0.7 and 3.5 mn thick, respectively. The wavelengths at which εL becomes equal to unity for those samples are marked with two other arrows.

appear to be experimentally verified. As it can be seen from Figure 6 the shift of the maximum position observed on changing the sample thickness corresponds to the changes of the absorption coefficient within the long wavelength tail of the $n\pi^*$ absorption (note that at room temperature no structure due to $n\pi^*$ transition can be observed in crystal absorption spectra). A difference between the spectra of positive and negative photocurrent is also readily understood.

The temperature dependences of the photocurrent presented in Figure 3 as well as the results presented by Itoh can be understood as follows. Within the range of strong $\pi\pi^*$ absorption, and below *ca* 450 nm there is no evidence of any wavelength dependence of the activation energy. This could be expected with a very simple idea of generation. It means that no matter what is the initially formed excited state, rapid internal conversion gives rise to the formation of the lower energy $n\pi^*$ singlet [this is the reason why phenazine shows no $\pi\pi^*$ fluorescence], and this $n\pi^*$ state is the one which should be regarded as the major precursor for photogenerated carriers. Thus no wavelength dependence of the "initial separation" or, in effect, the photocurrent activation energy should be expected. For longer wavelengths, however, the temperature dependence of the photocurrent reflects not only the changes of the photogeneration yield, but also changes of the relevant absorption coefficients. In this region, according to Figure 6 the absorption is no longer complete, so that sharpening of the $n\pi^*$ singlet absorption tail may give apparently much steeper temperature dependences of the photocurrent. It should be also added that in this spectral region currents due to detrapping of charges are of great importance. These are, however, dependent on the previous charging of a sample. This can be most easily seen for the triplet absorption region (Figure 4). Photocurrents in this region are primarily produced by interaction of triplet excitons with trapped holes. The fact that these photocurrents could be observed at room temperature and that they could still be seen a few hours after the charging treatment indicates that holes are very deeply trapped, and *ca* 1 eV is a reasonable estimate for the depth of the hole traps involved. The origin of this trap is unknown. It has to be remembered, however, that phenazine possesses rather high ionization potential making the phenazine crystal accessible to hole trap formation by various impurities of lower ionization potentials (e.g. anthracene molecule would form *ca* 1 eV deep hole trap in phenazine lattice).

References

1. L. Onsager, *Phys. Rev.*, **54**, 554 (1938).
2. J. Noolandi and K. M. Hong, *J. Chem. Phys.*, **70**, 3230 (1979).
3. D. M. Pai and R. C. Enck, *Phys. Rev.*, **B11**, 5163 (1975).
4. J. Noolandi, J. B. Webb, and D. F. Williams, in preparation.
5. L. Goodman and R. W. Harrel, *J. Chem. Phys.*, **30**, 1131 (1959).
6. R. M. Hochstrasser, *J. Chem. Phys.*, **36**, 1808 (1962).
7. M. Kleinerman, L. Azarraga, and S. P. McGlynn, *J. Chem. Phys.*, **37**. 1825 (1962).
8. U. Itoh and H. Anzai, *J. Phys. Soc. Japan*, **25**, 1197 (1968).
9. U. Itoh, Photoconduction in anthracene and anthracene-analogue compounds, Researches of the Electrotechnical Laboratory No. 752, Tokyo 1975.
10. R. H. Clarke and R. M. Hochstrasser, *J. Chem. Phys.*, **47**, 1915 (1967).
11. A. Fort and A. Coret, *Phys. Stat. Solidi* (*b*), **83**, 599 (1977).
12. R. M. Hochstrasser and C. Marzzacco, *J. Chem. Phys.*, **49**, 971 (1968).
13. K. H. Probst and N. Karl, *Phys. Stat. Solidi* (*a*), **27**, 499 (1975).

Appendix

To describe qualitatively the photocurrent modified by the existence of secondary recombination we shall consider a steadystate balance of the form:

$$\frac{\partial n}{\partial t} = 0 = \eta \varepsilon I_0 e^{-\varepsilon x} - \frac{n}{\tau_R(x)} - \frac{n}{t_f(x)} \tag{1}$$

where ε is the absorption coefficient, η stands for the generation efficiency (and is considered to be independent of ε) and I_0 is the incident light intensity. $\tau_R(x)$ is the recombination lifetime. Since τ_R is proportional to the reciprocal of the concentration of recombination centres, then we can write

$$\tau_R = \alpha \varepsilon^{-1} e^{\varepsilon x} \tag{2}$$

i.e., we consider the concentration of trapped holes to be proportional to the number of electron-hole pairs produced at the depth x; $t_f(x)$ is given by

$$t_f(x) = \begin{cases} \dfrac{L - x}{\mu F} \text{ for negative photocurrent} \\[2ex] \dfrac{x}{\mu F} \text{ for positive photocurrent} \end{cases} \tag{3}$$

and is the lifetime of the moving negative carrier in absence of recombination provided that it was generated at the depth x. More correctly, the term $n/t_f(x)$ should be substituted by $\mu(\partial(n(x)F(x))/\partial x)$ where F stands for the electric field strength and μ for mobility of carriers. Extracting $n(x)$ from (1) and integrating the expression from 0 to L-the crystal thickness, we obtain an estimate of the value of the current

$$J \propto \int_0^L n(x)\mathrm{d}x = \eta I_0 \int_0^L \frac{\varepsilon e^{-\varepsilon x}}{\dfrac{\varepsilon e^{-\varepsilon x}}{\alpha} + \dfrac{1}{t_f}} \mathrm{d}x \tag{4}$$

Thus

$$J \propto \begin{cases} \displaystyle\int_0^1 \frac{z e^{-zy}\,\mathrm{d}y}{\dfrac{z e^{-zy}}{A} + \dfrac{1}{1 - y}} \quad \text{for negative photocurrent} \\[4ex] \displaystyle\int_0^1 \frac{z e^{-zy}\,\mathrm{d}y}{\dfrac{z e^{-zy}}{A} + \dfrac{1}{y}} \text{ for positive photocurrent} \end{cases} \tag{5}$$

where the parameters are

$$y = \frac{x}{L}, \tag{6}$$

$$z = \varepsilon L \tag{7}$$

and A expresses the recombination probability as

$$A = \frac{\alpha L}{\mu F} \tag{8}$$

Expressions (1–5) have been used to calculate curves displayed in Figure 5.